



Extracting the surface tension of soft gels from elastocapillary wave behavior

Journal:	<i>Soft Matter</i>
Manuscript ID	SM-ART-05-2018-001027.R2
Article Type:	Paper
Date Submitted by the Author:	03-Jul-2018
Complete List of Authors:	Shao, Xingchen; Clemson University, Mechanical Engineering Saylor, John; Clemson University, Mechanical Engineering Bostwick, Joshua; Clemson University, Mechanical Engineering

Extracting the surface tension of soft gels from elastocapillary wave behavior

X. Shao¹, J.R. Saylor¹, and J.B. Bostwick^{1,*}

July 10, 2018

Mechanically-excited waves appear as surface patterns on soft agarose gels. We experimentally quantify the dispersion relationship for these waves over a range of shear modulus in the transition zone where the surface energy (capillarity) is comparable to the elastic energy of the solid. Rayleigh waves and capillary-gravity waves are recovered as limiting cases. Gravitational forces appear as a pre-stress through the self-weight of the gel and are important. We show the experimental data fits well to a proposed dispersion relationship which differs from that typically used in studies of capillary to elastic wave crossover. We use this combined theoretical and experimental analysis to develop a new technique for measuring the surface tension of soft materials, which has been historically difficult to measure directly.

1 Introduction

Capillary instabilities in Newtonian fluids are widely used in industrial processes such as spray cooling, inkjet printing/rapid prototyping, turbulent mixing, and the float-zone method of crystal growth. Recent interest in bio-printing technologies such as cell printing and tissue engineering use these basic principles but adapted to bioinks^{1,2}, which are typically hydrogels with complex rheologies characterized by non-trivial elasticity that are capable of sustaining biological function. In this paper, we report the experimental observation of parametrically-excited surface waves on soft agarose gels and characterize the dispersion relationship over a large range of shear modulus. We present a new technique for measuring the surface tension of soft hydrogels.

Traditional surface tension measurement techniques, such as the Du Nuoy tensiometer or Wilhelmy plate, work well for liquid interfaces but are difficult to apply to soft hydrogels. Alternative methods measure the solid surface tension as a fitting parameter that characterizes an observed property of the interface, such as the geometry the wetting ridge³, the shape of the solid meniscus during indentation^{4,5}, or the statistical distribution of delay times during fracture nucleation⁶. Notably, a bridge tensiometer has recently been used to measure the surface tension of yield stress materials, such as Carbonpol gel. Specifically, the surface tension is extracted from an elastoplastic model that delineates elastic from yield stress effects⁷. Here we establish a technique which uses the dispersion relationship of mechanically-excited surface waves to measure the solid surface tension of soft gels. Our technique is distinguished by its simplicity, as our experiments use equipment

that is both common and inexpensive.

Recent work has shown that surface tension forces can dominate the dynamics of soft gels, leading to Rayleigh-Taylor⁸ and Plateau-Rayleigh⁹ instabilities. Capillary-gravity waves travel on a liquid/gas interface endowed with surface tension^{10,11} and obey the dispersion relationship

$$\omega = \sqrt{gk + \frac{\sigma}{\rho}k^3}, \quad (1)$$

where ω is the angular frequency, k is the wavenumber, g is the gravitational constant, σ is the liquid/gas surface tension, and ρ is the liquid density. Capillary-gravity waves have been well-studied because they are relevant to numerous technologies that occur over many length scales; e.g. gravity waves are responsible for momentum exchange between atmospheric layers¹², whereas capillary waves are utilized in pulmonary drug delivery systems such as nebulizers¹³ and are prevalent in wave dissipation (breaking)¹⁴ and gas/momentum exchange^{15–18} in oceanography.

In contrast to capillary-gravity waves, Rayleigh surface waves on linear elastic solids are non-dispersive or have constant wave speed¹⁹. The dispersion relationship is given by

$$\omega = C\sqrt{\frac{\mu}{\rho}}k \quad (2)$$

where μ is the shear modulus, and can be used to measure shear elasticity in solids^{20,21}. The constant C encompasses properties such as material compressibility and finite-depth effects. For reference, $C = 0.955$ for incompressible materials of semi-infinite extent. The non-dispersive nature of Rayleigh waves is used in non-destructive material testing to identify cracks^{22,23}, geotechnical analysis of underwater²⁴ and sub-surface²⁵ features, and the food science industry for quality

¹Department of Mechanical Engineering, Clemson University, Clemson, SC 29634, USA.

* jbostwi@clemson.edu

control and sorting^{26,27}, and in magnetic resonance elastography (MRE)^{28,29}.

Waves on soft materials are known to possess properties of both capillary and elastic waves. The crossover from capillary to elastic waves has been experimentally observed in electrically-excited traveling waves on agarose gels^{30–32}, and in ultrasonically-excited soft viscoelastic layers³³. Observations, in general, match a predicted dispersion relationship derived from either an elastic³⁴ or fluid³⁵ based model, both of which include elastic and surface tension effects. More complex models for capillary waves that account for viscoelastic substrate effects have also been put forth^{36–38}. A historical perspective is given in the recent article by Monroy³⁹. For ultra-soft solids, the self-weight of the gel can become important as seen in gravity-driven instabilities⁴⁰ and the results we report here.

Herein we use Faraday waves to investigate the dispersion relationship of soft hydrogels and to study the transition from capillary to elastic waves. Faraday waves are formed at an interface by a parametric instability when the system is vibrated in the vertical direction, resulting in a wave having a frequency half that of the forcing frequency⁴¹. For Newtonian fluids, the literature on Faraday waves is vast (see review in Miles & Henderson⁴²), whereas that for viscoelastic liquids is comparatively small^{43–47}. Notably, Kumar⁴⁸ studied this system analytically, exploring the relative strengths of elastic and viscous forces on the onset amplitude and showing the existence of harmonic forcing (not the expected subharmonic) when the elastic forces are strong. However, to the best of our knowledge, Faraday waves have not been used as a means to investigate the dispersion relationship for soft hydrogels.

We begin this paper by outlining our experimental protocol for exciting and characterizing surface waves on soft agarose gels with shear moduli ranging from $\mu = 1\text{Pa}–260\text{Pa}$. Our experiments yield a dispersion relationship for each shear modulus from which we capture the transition from capillarity-dominated to elasticity-dominated dynamics. We then develop a theoretical dispersion relationship and show how to extract the solid surface tension^{3,49,50} from our experimental data. This new technique is a relatively simple way to measure the surface tension of soft hydrogels. We conclude by discussing the relevance of our experimental technique and analysis to technologies that concern the dynamics of soft hydrogels.

2 Experimental procedure

We investigate Faraday waves on soft agarose gels using the experimental setup shown in Figure 1. A 9 cm \times 9.5 cm plexiglass container filled with agarose gel is vertically driven by a shaker over a range of driving frequencies $f_d = 60–200\text{Hz}$. The shaker is driven by a function generator/amplifier combination. Surface instabilities with square wave symmetry,

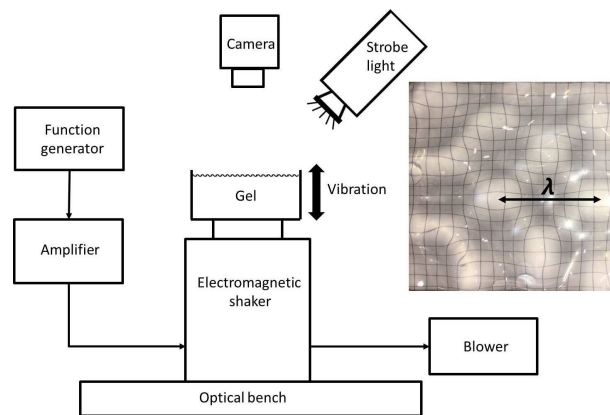


Fig. 1 Schematic of the experimental apparatus with typical surface wave image with wavelength λ .

shown in Figure 1, were observed above a threshold forcing amplitude. Images are captured using a strobe light and digital camera mounted above the container.

Our hydrogels are prepared by dissolving agarose powder (Sigma Aldrich Type VI-A) in deionized water using the method of Tokita⁵¹; the liquid mixture is kept at 90°C for 1 hour before being cast into the container and allowed to cool at room temperature overnight. We choose a gel height $h = 24\text{mm}$ to minimize finite-size depth effects, such that the solid can be treated as semi-infinite. We investigate concentrations in the range $\phi = 0.06–0.275\%w$, which is above the gel transition $\phi_c = 0.013\%w$ at 20°C and corresponds to a shear modulus $\mu = 1–260\text{Pa}$. The complex modulus $G = G' + iG''$ characterizes the rheology of agarose gels, which are known to have a loss modulus G'' that is many orders of magnitude smaller than the storage modulus G' over the range of frequencies used in our experiments^{30,51}. This implies that our gels behave as a linear elastic solid for the purposes of this study.

Surface waves were observed having a frequency f_o where $f_o = f_d/2$, as is expected for Faraday waves^{41,52}. A strobe light is used to ‘freeze’ the wave surface, allowing us to obtain images at a fixed phase of the wave cycle, by setting the strobe frequency to f_o . Herein, we focus on the dispersion relationship and will refer to the wave frequency as $f \equiv f_o$. A fast Fourier Transform (FFT) technique was used to analyze the spatial structure of the wave pattern, from which we extract an averaged wavelength λ . To eliminate edge wave effects, we crop the image to 0.8 times its original size.

3 Experimental results

Our experimental protocol allows us to extract the dispersion relationship from our data (f, λ) , as it depends upon the shear modulus μ . Herein we present our results in terms of angular

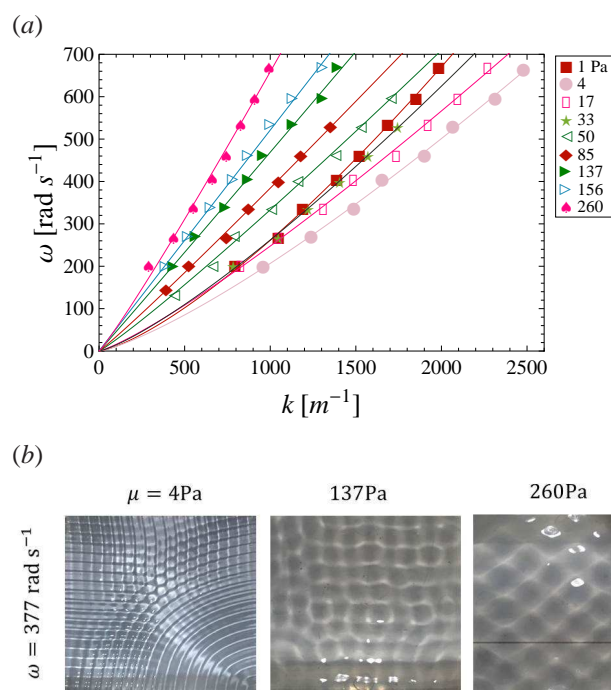


Fig. 2 (a) Dispersion relationships plotting angular frequency ω against wavenumber k for a range of shear modulus μ . Symbols are experimental data and lines are best fit power-laws. (b) Typical surface waves for $\omega = 377 \text{ rad s}^{-1}$, and $\mu = 4, 137,$ and 260 Pa .

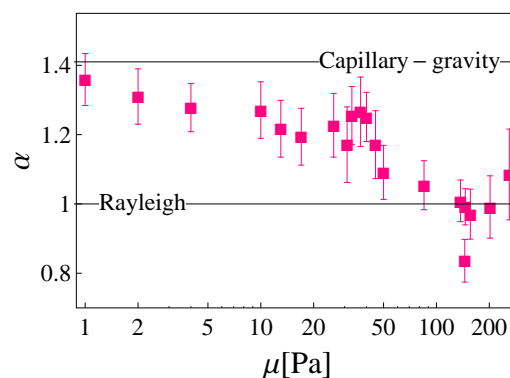


Fig. 3 Power law exponent α fitted to experimental data against shear modulus μ with limiting cases for Rayleigh $\alpha = 1$ and capillary-gravity $\alpha = 1.41$ waves annotated. Error bars represent 95% confidence intervals.

frequency $\omega \equiv 2\pi f$ and wavenumber $k \equiv 2\pi/\lambda$ to compare with the dispersion relationships for capillary-gravity (1) and Rayleigh (2) waves. For our ultra-soft agarose gels, we expect the dynamics to lie between these two extremes^{30,31}. Our focus is on the role of the substrate elasticity μ .

Figure 2(a) is a plot of the dispersion relationship, ω against k , for the range of shear moduli μ explored here. Typical surface wave patterns are shown in Figure 2(b) for fixed frequency ω and three values of modulus μ . The dispersion curves show the frequency ω is monotonic with wavenumber k , whereas the curves are non-monotonic with shear modulus μ . This can be seen by ordering the curves by μ as the graph is traversed from left to right; note especially that the experimental data for $\mu = 1 \text{ Pa}$ lies to the left of the $\mu = 4 \text{ Pa}$ curve. This observation highlights the interplay between elasticity and capillarity, as well as the prominent role of surface tension in gels with small μ .

We fit the raw experimental data to a power-law having the form $\omega = Ck^\alpha$, to gain insight into the transition from capillary-dominated to elasticity-dominated regimes. These curves are overlaid on the experimental data in Figure 2(a). Figure 3 is a plot of the power-law exponent α against shear modulus μ with vertical bars equal to the 95% confidence interval for each data point. For reference, capillary-gravity waves have a power-law exponent $\alpha = 1.41$ and Rayleigh waves $\alpha = 1$ over this range of frequencies. As seen in Figure 3, the majority of data lies within these bounding curves implying that both surface tension and elasticity are important to understand the dynamics. Note that gravity, which manifests itself through the self-weight of the gel, is an important factor in the dispersion relationship—pure capillary waves would have $\alpha = 1.5$. In the limit $\mu \rightarrow 0 \text{ Pa}$, the waves behave as capillary-gravity waves, whereas for $\mu > 85 \text{ Pa}$, the

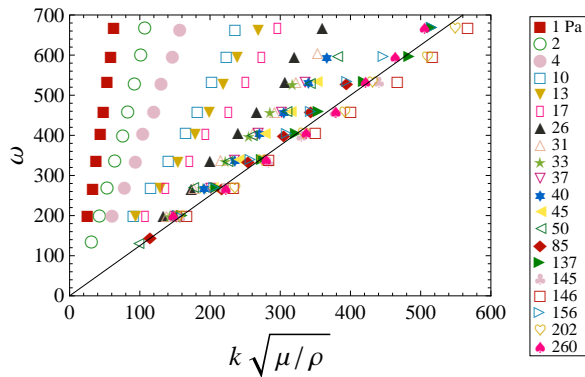


Fig. 4 Rayleigh wave scaling (Eq. 2): angular frequency ω against $k\sqrt{\mu/\rho}$ shows a collapse of experimental data for shear modulus $\mu > 85$ Pa. A best fit line for $\mu > 85$ Pa is plotted to guide the eye.

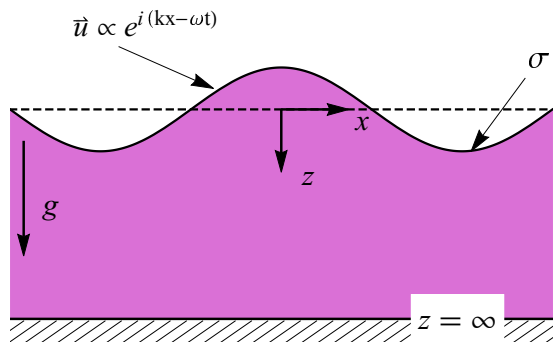


Fig. 5 Definition sketch. A linear elastic solid occupies a semi-infinite half-space in the presence of a gravitational field g and has an interface $z = 0$ endowed with surface tension σ that is perturbed by a wave $e^{i(kx-\omega t)}$.

exponent $\alpha = 1$ within the 95% confidence interval (with the exception of one outlier) indicating Rayleigh wave behavior. In Figure 4, we rescale the experimental data with respect to the form of the Rayleigh wave dispersion relationship (2) and show a collapse of the data for $\mu > 85$ Pa, implying that surface tension forces do not affect the dynamics in this “high” μ regime.

So, while surface tension forces seem to become unimportant with sufficiently large μ , the converse cannot be said for elasticity effects which are important even for small μ . For example, as shown in Figure 3, it is not until $\mu = 1$ Pa that α approaches 1.41.

4 Theoretical model

We are interested in developing a closed-form dispersion relationship to compare with our experiments, because existing

theories of elastocapillary waves^{34,35} involve the solution of a complex nonlinear characteristic equation. We briefly sketch the details of our model, which builds upon the work of Onodera and Choi³⁴.

Consider a linear elastic solid that occupies a semi-infinite half-space and deforms due to its self-weight (gravitational constant g). The gel surface is endowed with surface tension σ and perturbed by a wave of the form $e^{i(kx-\omega t)}$, as shown in Figure 5. The displacement field $\mathbf{u}(x, z, t) \equiv (u, w)$ obeys the elastodynamic Navier equations,

$$\rho \frac{\partial^2 \mathbf{u}}{\partial t^2} = (\lambda + \mu) \nabla(\nabla \cdot \mathbf{u}) + \mu \nabla^2 \mathbf{u} \quad (3)$$

where λ, μ are the Lamé parameters. Continuity of stress τ is enforced at the free surface $z = 0$;

$$\tau_{xz} = 0, \quad \tau_{zz} = -\sigma \frac{\partial^2 w}{\partial x^2} + \rho g w. \quad (4)$$

The first equation ensures the interface is free of shear stress, while the second is the Young-Laplace equation which relates the normal stress to the linearized mean curvature. The $\rho g w$ term is the disturbance to the pre-stress due to the gravitational body force or self-weight. Lastly, we require our solution to be bounded $|\mathbf{u}| \rightarrow 0$ as $z \rightarrow \infty$.

To construct a solution to the field equations (3)–(4), we use the Helmholtz decomposition theorem to write the displacement field

$$\mathbf{u} = \nabla \phi + \nabla \times \boldsymbol{\psi} \quad (5)$$

in terms of the scalar potential ϕ and vector potential $\boldsymbol{\psi} = \psi \hat{j}$. Equivalently, $\mathbf{u} = (u, w) = (\phi_x - \psi_z, \phi_z + \psi_x)$ in component form. Sometimes ϕ and ψ are referred to as the compressional and shear wave potentials, respectively. Substituting (5) into (3) delivers a set of uncoupled equations,

$$\frac{\partial^2 \phi}{\partial t^2} = \alpha^2 \nabla^2 \phi, \quad \frac{\partial^2 \psi}{\partial t^2} = \beta^2 \nabla^2 \psi, \quad (6)$$

where $\alpha \equiv \sqrt{(\lambda + 2\mu)/\rho}$ and $\beta \equiv \sqrt{\mu/\rho}$. Normal modes $e^{i(kx-\omega t)}$ taking the form of steady waves propagating in the x -direction are assumed with k the wavenumber and ω the wave frequency. The solution of (6) is then given by

$$\phi = A e^{-\gamma z} e^{i(kx-\omega t)}, \quad \psi = B e^{-\delta z} e^{i(kx-\omega t)}, \quad (7)$$

where $\gamma \equiv \sqrt{k^2 - \omega^2/\alpha^2}$ and $\delta \equiv \sqrt{k^2 - \omega^2/\beta^2}$ and (A, B) are unknown coefficients to be determined from the stress boundary conditions (4). Substituting (7) into the displacement form of the stress boundary conditions (4),

$$\mu \left(\frac{\partial u}{\partial z} + \frac{\partial w}{\partial x} \right) = 0, \quad \lambda \frac{\partial u}{\partial x} + (\lambda + 2\mu) \frac{\partial w}{\partial z} = -\sigma \frac{\partial^2 w}{\partial z^2} + \rho g w, \quad (8)$$

gives a set of linear equation for the constants A, B ,

$$\begin{bmatrix} i2k\gamma & 2k^2 - \frac{\omega^2}{\beta^2} \\ 2k^2 - \frac{\omega^2}{\beta^2} + \frac{\gamma}{\beta^2} \left(\frac{\sigma k^2}{\rho} + g \right) & -i2k\delta - i\frac{k}{\beta^2} \left(\frac{\sigma k^2}{\rho} + g \right) \end{bmatrix} \begin{bmatrix} A \\ B \end{bmatrix} = \begin{bmatrix} 0 \\ 0 \end{bmatrix}. \quad (9)$$

The resulting characteristic equation

$$4\sqrt{1 - \frac{1-2\nu}{2(1+\nu)}c^2} \sqrt{1-c^2} - (2-c^2)^2 + c^2 \sqrt{1 - \frac{1-2\nu}{2(1+\nu)}c^2} \left(L_e k + \frac{1}{L_g k} \right) = 0. \quad (10)$$

is written with respect to the scaled Rayleigh wave speed $c \equiv \sqrt{\rho/\mu}(\omega/k)$, Poisson ratio ν , elastocapillary length $L_e = \sigma/\mu$ and elastogravity length $L_g = \mu/\rho g$.

The agarose gels we use in our experiments can be considered incompressible $\nu = 1/2$ which allows the following simplification of the characteristic equation (10),

$$4\sqrt{1-c^2} - (2-c^2)^2 + c^2 \left(L_e k + \frac{1}{L_g k} \right) = 0. \quad (11)$$

Note that (11) is a nonlinear equation for the wave speed c that depends upon the wavenumber k , elastocapillary length L_e and elastogravity length L_g . Assuming our agarose gels have solid surface tension close to that of water $\sigma = 72\text{mN/m}$, we estimate $L_e \sim 10^{-2} - 10^{-4}\text{m}$ in our experiments. Similarly, $L_g \sim 10^{-2} - 10^{-4}\text{m}$ but with the opposite trend of L_e implying there is range of shear moduli where $L_g \sim L_e$. Equating $L_g = L_e$ yields the critical shear modulus $\mu \approx 26\text{Pa}$, which is clearly in the transition zone between capillary-gravity and Rayleigh waves shown in Figure 3. A simple scale analysis between the surface wavelength $1/k$ and the elastocapillary length L_e gives capillarity-dominated $L_e \gg 1/k$ and elasticity-dominated $1/k \gg L_e$ regimes. In terms of our data set, the observed wavelengths for $\mu = 1\text{Pa}$ are all an order of magnitude smaller than L_e and are capillary waves, whereas for $\mu > 85\text{Pa}$ the observed wavelengths are an order of magnitude larger than L_e and are Rayleigh waves (cf. Figure 2). These scaling arguments are consistent with the transition zone $1 < \mu < 85\text{Pa}$ shown in Figure 3. In the transition zone, both capillarity and elasticity affect the dynamics in a way that cannot be predicted a priori from scale analysis.

The disadvantage of (11) is that it is nonlinear and the dispersion relationship must be computed numerically. We seek to develop an approximate solution to more simply compare and analyze our experiments. We do this by series expanding Eq. (11) about $\mu = \infty$, keeping the lowest order terms, and solving the resulting equation to deliver the dispersion rela-

tionship

$$\omega = \sqrt{\frac{2}{3}gk + \frac{2}{3}\frac{\sigma}{\rho}k^3 + \frac{4}{3}\frac{\mu}{\rho}k^2}, \quad (12)$$

We note that Figure 4 shows the experimental data collapses upon scaling with the Rayleigh wave dispersion, Eq. (2), for large $\mu > 85\text{Pa}$ and the slope of that line is approximately 1.17, which is close to our predicted coefficient $\sqrt{4/3} \approx 1.15$, thus validating Eq. (12). For all our experimental data with the exception of $\mu = 1\text{Pa}$, $L_e k \leq O(1)$ and we expect Eq. (12) to be faithful. For $\mu = 1\text{Pa}$, however, $L_e k \approx 10$ and we might expect Eq. (12) to breakdown at this $L_e k \gg 1$ limit. This is confirmed by the fact that Eq. (12) does not recover the $\mu \rightarrow 0$ limit, Eq. (1). The advantage of Eq. (12) is a readily available closed-form solution for use in interpreting our experiments.

We fit the experimental data to (12) treating surface tension σ as a parameter. Figure 6 is a plot of the resulting surface tension σ versus shear modulus μ . The experimental data completely collapses in this case, as shown in Figure 7, which validates the use of our proposed dispersion relationship (12) in determining the surface tension of soft gels. The average value over the entire range of μ produces $\sigma = 45.6\text{mN/m}$ (cf. Figure 6). For reference, we show how the experimental data scales with the dispersion relationship (12) for this fixed surface tension value in the Appendix (Figure 8). Figure 6 shows the predicted σ values tend to become more scattered for $\mu > 137\text{Pa}$, which is firmly in the Rayleigh wave regime (cf. Figs 3,4) where the particular value of σ is largely irrelevant because of the dominant elastic forces. Other potential sources of scatter may include edge effects associated with large wavelength patterns in this regime and uncertainty in the shear modulus of our stiffest gel ($\mu = 260\text{Pa}$) which we have extrapolated from the data of Tokita and Hikichi⁵¹. Finally, we note the relatively large surface tension $\sigma = 83.2\text{mN/m}$ predicted for our softest gel $\mu = 1\text{Pa}$, which we attribute to the range of validity of Eq. (12) mentioned above. We conclude that (12) does a good job of predicting our experimental observations allowing us to extract the surface tension of soft gels, and may serve as a useful tool to other workers in this field.

5 Discussion

We have conducted experiments on mechanically-excited surface waves on soft agarose gels and characterized the dispersion relationship over a large range of shear moduli. Capillarity can dominate the dynamics for soft materials and our results capture the transition from capillary-gravity to Rayleigh waves as it depends upon the shear modulus. In addition, we have developed a new technique to measure the surface tension of soft hydrogels by using a theoretical dispersion relationship for elastocapillary waves. We expect this new mea-

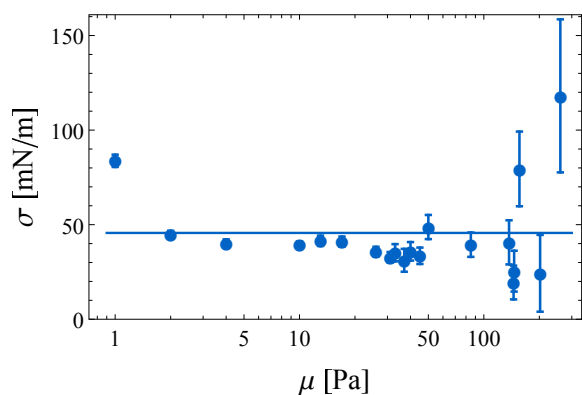


Fig. 6 Predicted surface tension σ [mN/m] against shear modulus μ [Pa] by fitting the dispersion relationship (12) to the experimental data. The average value over the entire range of μ gives $\sigma = 45.6$ mN/m. Error bars represent 95% confidence intervals.

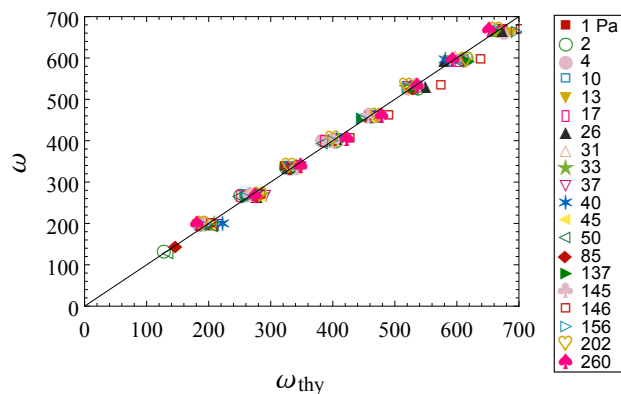


Fig. 7 Elastocapillary wave scaling: angular frequency ω against proposed dispersion relationship ω_{thy} . Eq. 12, shows a collapse of experimental data for all shear modulus explored here.

surement technique, as well as our analysis of the dynamics of soft materials, to be highly relevant to a number of other technologies and to be useful to researchers working in the area of soft hydrogels.

Capillary instabilities in Newtonian fluids are widely used in industrial processes such as spray cooling, inkjet printing/rapid prototyping, turbulent mixing, and the float-zone method of crystal growth, all of which operate using the basic physical principles of the respective instabilities. For example, the formation of aerosols using vibrating transducers delivers drops with size related to the capillary frequency. Recent interest in technologies such as cell printing and tissue engineering use these basic principles but adapted to viscoelastic materials, such as bioinks^{1,2}, which are typically hydrogels with complex rheologies (i.e. both liquid and solid properties)⁵³. The agarose gels we use in our experiments are also used in cell printing, making our results potentially applicable to the dynamics of pinch-off in single cell epitaxy⁵³.

Surface tension forces are important for gels with shear modulus $\mu < 137$ Pa in our experiments, whereas elasticity affects the dispersion relationship for even our softest gels. In contrast, solid capillarity⁵⁴ can affect elastocapillary or soft wetting phenomena in much stiffer substrates; e.g. droplet spreading on silicone gel substrates with $\mu \sim 3$ kPa can exhibit rich behaviors, such as stick-slip and stick-breaking motions, which are linked to the formation of a wetting ridge at the three-phase contact-line⁵⁵. Viscoelastic effects can be expected to further complicate the dynamics of pattern formation in our experiments when the gel has a complex rheology. Future experiments could investigate the ability to control a dominant mode in viscoelastic gels for precise, robust and repeatable cell printing.

Acknowledgements

We wish to thank Jon Brownfield for assisting in the development of the numerical algorithm used to extract wavelengths from the experimental images. JBB acknowledges support from NSF Grant CBET-1750208.

A Comparison to experimental data for average surface tension value

In Figure 7 we showed how the proposed dispersion relationship (12) collapsed our entire data set when treating the surface tension as an unknown parameter. The average value of surface tension over the entire data set was computed to be 45.6 mN/m. Figure 8 plots the experimental data ω against the dispersion relationship ω_{thy} (12) using this value of surface tension, i.e. no fitting parameter. As shown, the comparison is worse than Figure 7, where we compute surface tension for

each data set, but still does a reasonable job of reproducing the experimental results. The only significant exceptions are the limiting cases of $\mu = 1\text{Pa}$ and 260Pa , where the predicted surface tension is furthest from that average value (cf. Figure 6).

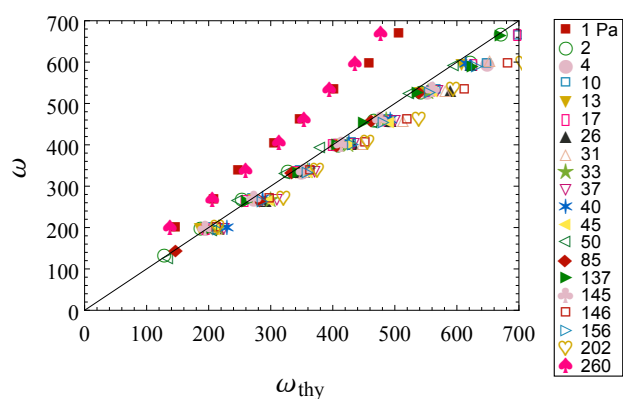


Fig. 8 Angular frequency ω against proposed dispersion relationship ω_{thy} , Eq. 12, using the average surface tension value $\sigma = 45.6\text{mN/m}$ for all μ .

References

- S. Ji and M. Guvendiren, *Frontiers in bioengineering and biotechnology*, 2017, **5**, year.
- R. Suntornnond, J. An and C. K. Chua, *Macromolecular Materials and Engineering*, 2016.
- R. W. Style, R. Boltyskiy, Y. Che, J. Wettlaufer, L. A. Wilen and E. R. Dufresne, *Physical review letters*, 2013, **110**, 066103.
- Q. Xu, R. W. Style and E. R. Dufresne, *Soft matter*, 2018, **14**, 916–920.
- Q. Xu, K. E. Jensen, R. Boltyskiy, R. Sarfati, R. W. Style and E. R. Dufresne, *Nature communications*, 2017, **8**, 555.
- M. Grzelka, J. B. Bostwick and K. E. Daniels, *Soft Matter*, 2017, **13**, 2962–2966.
- L. Jørgensen, M. Le Merrer, H. Delanoë-Ayari and C. Barentin, *Soft Matter*, 2015, **11**, 5111–5121.
- S. Mora, T. Phou, J.-M. Fromental and Y. Pomeau, *Physical review letters*, 2014, **113**, 178301.
- S. Mora, C. Maurini, T. Phou, J.-M. Fromental, B. Audoly and Y. Pomeau, *Physical review letters*, 2013, **111**, 114301.
- L. Rayleigh, *Proceedings of the London Mathematical Society*, 1877, **s1-9**, 21–26.
- H. Lamb, *Hydrodynamics*, Cambridge University Press, Cambridge, UK, 1932.
- D. C. Fritts and M. J. Alexander, *Reviews of geophysics*, 2003, **41**, year.
- H. D. Smyth and A. J. Hickey, *Controlled pulmonary drug delivery*, Springer, 2011.
- W. K. Melville and P. Matusov, *Nature*, 2002, **417**, 58–63.
- W. Melville, *Annual review of fluid mechanics*, 1996, **28**, 279–321.
- L. Deike, S. Popinet and W. K. Melville, *Journal of Fluid Mechanics*, 2015, **769**, 541–569.
- J. R. Saylor, *Tellus*, 1999, **51B**, 616–628.
- J. R. Saylor and R. A. Handler, *Exp. Fluids*, 1999, **27**, 332–338.
- L. Rayleigh, *Proceedings of the London Mathematical Society*, 1885, **1**, 4–11.
- J. Brum, S. Catheline, N. Benech and C. Negreira, *The Journal of the Acoustical Society of America*, 2008, **124**, 3377–3380.
- X. Zhang and J. F. Greenleaf, *The Journal of the Acoustical Society of America*, 2007, **122**, 2522–2525.
- E. Lean and C. Powell, *Applied Physics Letters*, 1971, **19**, 356–359.
- B. Masserey, *PhD thesis*, 2006.
- B. A. Luke and K. H. S. II, *Journal of Geotechnical and Geoenvironmental Engineering*, 1998, **124**, 523–531.
- C. B. Park, R. D. Miller and J. Xia, *Geophysics*, 1999, **64**, 800–808.
- T. Ikeda, P.-K. Choi, T. Ishii, I. Arai and M. Osawa, *Journal of Food Engineering*, 2015, **160**, 28–33.
- S. Hitchman, K. van Wijk and Z. Davidson, *Postharvest Biology and Technology*, 2016, **121**, 71–77.
- R. Muthupillai, D. Lomas, P. Rossman, J. F. Greenleaf *et al.*, *Science*, 1995, **269**, 1854.
- A. Manduca, T. E. Oliphant, M. Dresner, J. Mahowald, S. A. Kruse, E. Amromin, J. P. Felmlee, J. F. Greenleaf and R. L. Ehman, *Medical image analysis*, 2001, **5**, 237–254.
- F. Monroy and D. Langevin, *Physical review letters*, 1998, **81**, 3167.
- P.-K. Choi, E. Jyounouti, K. Yuuki and Y. Onodera, *The Journal of the Acoustical Society of America*, 1999, **106**, 1591–1593.
- P.-K. Choi, E. Jyounouti, K. Yamamoto and K. Takagi, *Japanese Journal of Applied Physics*, 2001, **40**, 3526.
- M. Tinguely, M. G. Hennessy, A. Pommella, O. K. Matar and V. Garbin, *Soft Matter*, 2016, **12**, 4247–4256.
- Y. Onodera and P.-K. Choi, *The Journal of the Acoustical Society of America*, 1998, **104**, 3358–3363.
- J. Harden, H. Pleiner and P. Pincus, *The Journal of chemical physics*, 1991, **94**, 5208–5221.
- M. L. Henle and A. J. Levine, *Physical Review E*, 2007, **75**, 021604.
- Y. Ohmasa and M. Yao, *Physical Review E*, 2011, **83**, 031605.
- J. Kappler and R. R. Netz, *EPL (Europhysics Letters)*, 2015, **112**, 19002.
- F. Monroy, *Advances in Colloid and Interface Science*, 2017, 4–22.
- S. Mora, T. Phou, J.-M. Fromental, L. M. Pismen and Y. Pomeau, *Phys. Rev. Lett.*, 2010, **105**, 214301.
- M. Faraday, *Philosophical transactions of the Royal Society of London*, 1831, **121**, 299–340.
- J. Miles and D. Henderson, *Annual Review of Fluid Mechanics*, 1990, **22**, 143–165.
- H. W. Müller and W. Zimmermann, *Europhysics Letters*, 1999, **45**, 169–174.
- C. Wagner, H. Müller and K. Knorr, *Physical review letters*, 1999, **83**, 308.
- P. Ballesta and S. Manneville, *Phys. Rev. E*, 2005, **71**, 026308.
- C. Cabeza and M. Rosen, *International Journal of Bifurcation and Chaos*, 2007, **17**, 1599–1607.
- P. Ballesta, M. P. Lettinga and S. Manneville, *Soft Matter*, 2011, **7**, 11440–11446.
- S. Kumar, *Physics of Fluids*, 1999, **11**, 1970–1981.
- E. R. Jerison, Y. Xu, L. A. Wilen and E. R. Dufresne, *Phys. Rev. Lett.*, 2011, **106**, 186103.
- J. B. Bostwick, M. Shearer and K. E. Daniels, *Soft Matter*, 2014, **10**, 7361–7369.
- M. Tokita and K. Hikichi, *Phys. Rev. A*, 1987, **35**, 4329.
- T. B. Benjamin and F. Ursell, *Proceedings of the Royal Society of London A: Mathematical, Physical and Engineering Sciences*, 1954, pp. 505–515.
- U. Demirci and G. Montesano, *Lab on a chip*, 2007, **7**, 1139–1145.
- B. Andreotti and J. H. Snoeijer, *EPL (Europhysics Letters)*, 2016, **113**, 66001.
- S. Park, J. Bostwick, V. De Andrade and J. Je, *Soft Matter*, 2017, **13**, 8331–8336.